Volume 13, Issue 3, Page 154-160, 2024 https://doi.org/10.46810/tdfd.1491408 Research Article

BİNGÖL UNIVERSITY

Türk Doğa ve Fen Dergisi
Turkish Journal of Nature and Science
www.dergipark.gov.tr/tdfd

Investigation Of Friction Welding Dissimilar AISI 304 And AISI 1040 Steels

Zülküf BALALAN[1*], Mehmet YAZ[2], Sedat BULDAĞ[3]

[1] Bingöl University, Faculty of Engineering and Architecture, Mechanical Engineering, Bingöl, Türkiye
[2] Firat University, Vocational School Of Technical Sciences/Department Of Machinery And Metal Technologies/Machinery, Elazığ, Türkiye
[3] Bingöl University, Faculty of Engineering and Architecture, Mechanical Engineering, Bingöl, Türkiye
Zülküf BALALAN ORCID No: 0000-0001-5808-6263
Mehmet YAZ ORCID No: 0000-0002-5422-7433
Sedat BULDAĞ ORCID No: 0009-0000-3877-6320

**Corresponding author: zbalalan@bingol.edu.tr*

(Received: 28.05.2024, Accepted: 09.09.2024, Online Publication: 26.09.2024)

Keywords
Joining, Dissimilar steels, Microstructure, Tensile strength, Microhardness

Abstract: Friction time is one of the important parameters in friction welding. The effect of friction time on the mechanical and microstructural properties of the weld was investigated in the friction welding of AISI 304 and AISI 1040 steels. With the enhancement of friction time, the temperature at the welding region naturally increased. Increasing the friction time resulted in the formation of a stronger weld. The highest tensile strength of 755 MPa was found in the S3 weld sample made at the highest friction time of 9 seconds. An increase in the friction time also provided a significant increase in the weld tensile elongation. S2 and S3 weld samples were broken as ductile during the tensile test, while S1 weld sample was broken as a mixture of brittle and ductile. The highest microhardness value of approximately 310 HV was determined at the joint area of the S1 weld produced with the lowest friction time. Hardness at the weld interface slightly decreased with an increase in the friction time. The weld interface shape changed depending on the friction time.

Farklı AISI 304 Ve AISI 1040 Çeliklerinin Sürtünme Kaynağının Araştırılması

Anahtar Kelimeler
Birleştirme, Farklı çelikler, Mikroyapı, Çekme mukavemet Mikrosertlik

Öz: Sürtünme süresi sürtünme kaynağında önemli parametrelerden biridir. AISI 304 ve AISI 1040 çeliklerinin sürtünme kaynağında sürtünme süresinin kaynağın mekanik ve mikroyapısal özelliklerine etkisi araştırıldı. Sürtünme süresinin artmasıyla birlikte kaynak bölgesindeki sıcaklık da doğal olarak artmıştır. Sürtünme süresinin artırılması daha sağlam bir kaynak oluşumuyla sonuçlandı. En yüksek çekme gerilmesi 9 saniyelik en yüksek sürtünme süresinde yapılan S3 kaynak numunesinde 755 MPa olarak bulunmuştur. Sürtünme süresindeki artış, kaynağın çekme uzamasında da önemli bir artış sağladı. Çekme testi sırasında S2 ve S3 kaynak numuneleri sünek olarak kırılırken, S1 kaynak numunesi gevrek ve sünek karışımı olarak kırılmıştır. En düşük sürtünme süresiyle üretilen S1 kaynağının birleşim bölgesinde yaklaşık 310 HV ile en yüksek mikrosertlik değeri belirlendi. Kaynak arayüzündeki sertlik, sürtünme süresinin artmasıyla birlikte hafifçe azalmıştır. Kaynak ara yüzeyinin şekli sürtünme süresine bağlı olarak değişmiştir.

1. INTRODUCTION

Friction welding, a solid-state joining technique, generates heat through mechanical friction between the surfaces of workpieces without the use of external heat. When an external force is applied, the workpieces deform plastically, allowing materials that are similar or dissimilar to be joined without melting. Friction welding is a solid-state method as opposed to fusion welding, which is a melting process [1]. Since friction welding influences a small surface area, less stress, flaws, and material loss result, lowering the chance of welding problems and material effects [2]. Combining dissimilar materials would enable more efficient and economical constructions in many applications [3]. Many defects such as pores and intermetallic phases that seriously affect the weld quality seen in fusion welding techniques do not occur in solid-state welding techniques because

the materials are welded without melting [4]. Joining dissimilar materials via conventional fusion welding techniques is not practical because of the production of brittle and low melting intermetallics due to metallurgical incompatibility, broad melting point differences, thermal mismatch, etc. In these kinds of circumstances, friction welding is commonly used [5, 6]. Friction welding offers significant advantages including notable material savings, short manufacturing times, and the ability to join different metals or alloys [7]. For instance, even completely different AZ31B magnesium alloy and AISI 304 stainless steel were reported to be successfully welded by the solid-state technique [8, 9]. Friction welding parameters (friction time, rotation speed, friction pressure, etc.) have a significant effect on heat generation, material flow, microstructure, residual stress, and weld quality. The impact of each parameter is greatly affected by the materials that are joined [1]. Balalan and Ekinci [10] investigated the effect of rotation speed on the mechanical characteristics of the welds of the AISI 1040 parts via the friction welding method. They obtained the strongest weld with 400 MPa at 1500 rpm. Celik et al. [11] studied the joining of AISI 304 and AISI 1040 steels by friction welding and reported that joint strength is proportional to friction pressure and these steels can be reliably joined for industrial applications. Paventhan et al. [12] studied friction welding of AISI 1040 and AISI 304 steel and reported that friction time significantly affects the weld strength. Various material combinations such as aluminum alloy and magnesium alloy [13], aluminum and copper [14], magnesium alloy and stainless steel [15], and stainless steel and zinc [16] have been successfully joined using the friction welding process.

The impact of friction time, which is an important friction welding parameter in joining AISI 304 and AISI 1040 steels by friction welding, on the weld's mechanical and microstructural properties has not been much researched. Therefore, in this study, AISI 304 and AISI 1040 steels which are widely used in many applications were combined through the friction welding technique. The influence of friction time on macro and microstructure, tensile strength, and microhardness were investigated.

2. MATERIAL AND METHOD

The chemical composition of the materials produced by the cold drawing method used in the experiments is given in Table 1, and their mechanical properties are presented in Table 2.

Table 1. Chemical compositions of materials (wt.%)

Materials	C	Mn	Cr	S	Ni	P	Mo
AISI 1040	% 0,37-0,44	0.60-0.90	-	0.050	-	0.040	-
AISI 304	0,042	1.47	18.25	0.032	8.09	0.032	0.30

Table 2. Mechanical properties of materials

Materials	Yield Strength (MPa)	Tensile Strength (MPa)	Elongation (%)	Microhardness ($HV_{0.3}$)		
AISI 304	310	616	35	205	203	207
AISI 1040	361	600	25	149	152	156

The materials were lathe machined to 100x12mm and prepared for friction welding. The friction welding parameters used are given in Table 3. Friction welding processes were done on the continuously driven friction welding machine shown in Figure 1. Macro photography of welded joints is given in Figure 2.

Table 3. Friction welding variables

Experiment Samples	Number of Revolutions (rpm)	Friction Pressure (da. N/cm^2)	Friction Time (s)	Upset Pressure (da. N/cm^2)	Upset Time (s)
S1	2200	30	5	60	6
S2	2200	30	7	60	6
S3	2200	30	9	60	6

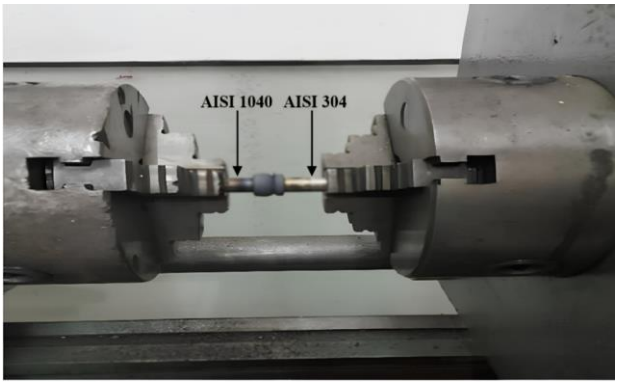

Figure 1. Friction welding process

Figure 2. Macro-photograph of the friction welds

After the friction welding process, the tensile strength test samples were produced from the welded joints according to TS 138 EN 895 the tensile strength test standard in Figure 3. Tensile strength tests were carried out on INSTRON brand tensile device. Three of each sample were subjected to tensile tests.

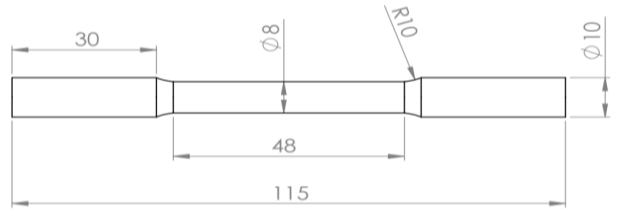

Figure 3. Dimension of the tensile strength test sample

Figure 4. Raynger 3i plus infrared temperature measurement device

To detect the microstructures of the welded samples, cross-section areas of the welds were sanded with sandpapers and then polished. After that, electrolytically etched using 47.6% HCl + 47.6% pure water + 4.8% NHO3 nitric acid solution. Then optical photographs were taken. In the microstructure analysis studies of the samples, the chemical content of the phase occurring in the weld area was determined by EDS. JEOL JSM6510 brand scanning electron microscope test device was used. To detect the intermetallic compounds formed, X-ray diffraction patterns (XRD) analysis from the etched cross-sectional area was performed using a Rigaku Ultima IV brand device. Microhardness measurement was carried out to detect the hardness in heat-affected zone (HAZ) and weld areas. Microhardness measurement was measured on the Vickers microhardness device, model THV-1D, by applying a load of 300 g and a waiting time of 10 seconds, with 0.5 mm intervals, as shown in Figure 5.

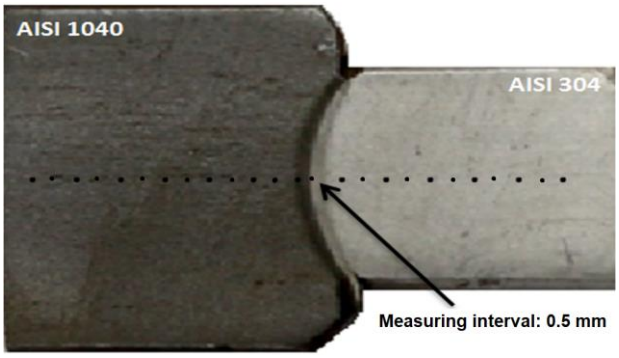

Figure 5. Microhardness measurement taken on the weld cross-section

3. RESULTS AND DISCUSSION

3.1. Measuring the Temperature of The Weld Region and Welded Sample Dimensions

Maximum temperatures measured from the welding areas are given in Table 4. As the friction time increased, the temperature increased slightly. Therefore, the flash material (the amount of material protruding from the interface) increased. The demonstration of measuring flash dimensions is shown in Figure 6. Flash widths and lengths, and length shortenings of the welded samples are given in Tables 5 and 6. The temperature at the weld region rose with a rise in the friction time, resulting in larger flash formation and sample length reduction.

Figure 6. Flash dimensions

Table 4. Weld area maximum temperature

Samples	Maximum Temperatures (°C)
S1	980
S2	1000
S3	1100

Table 5. Weld samples flash dimensions

Length	Material	S1	S2	S3
Flash Width (mm)	**AISI 1040**	5.01	6.55	7.24
	AISI 304	2.98	3.45	3.90
Flash Length (mm)	**AISI 1040**	18.87	20.06	20.50
	AISI 304	16.36	17.30	18.27

Table 6. Length reduction amounts of the weld samples

Samples	Shortening in length (mm)
S1	13.11
S2	16.15
S3	17.10

3.2. Metallographic Examination

Figure 7 shows the schematic demonstration of the weld cross-section. Four different zones were identified. The base material zone, heat-addected zone, deformed zone, and extremely deformed zone, which is within the deformation zone but shows structural differences. The heat-affected, deformed, and extremely deformed areas were determined to be larger on the AISI 1040 side. It is consistent with the literature that the size of these four defined regions varies depending on the process parameter [17].

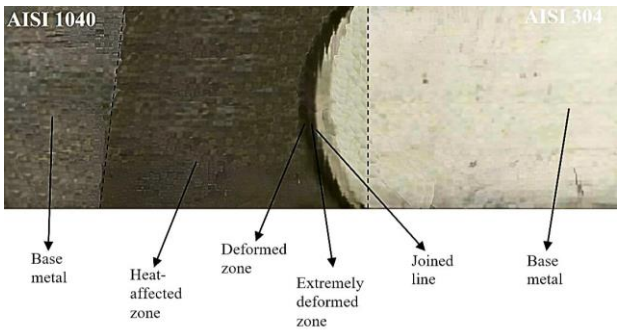

Figure 7. Schematic picture of the joint cross-section in friction welded samples

The SEM photograph of AISI 304 austenitic stainless steel and the AISI 1040 steel is given in Figure 8. As a source of austenitic stainless steel, chromium carbide precipitation occurs in some stainless steels such as 18/8 steel at a temperature in the temperature range of 450-850 °C. Since 90% of the chromium carbide formed consists of Cr by weight, even a very small amount of carbon at the grain boundary reduces the chromium level around the austenite grain excessively. When the

material remains in a corrosive area, corrosion occurs in the chromium-weakened grain [12].

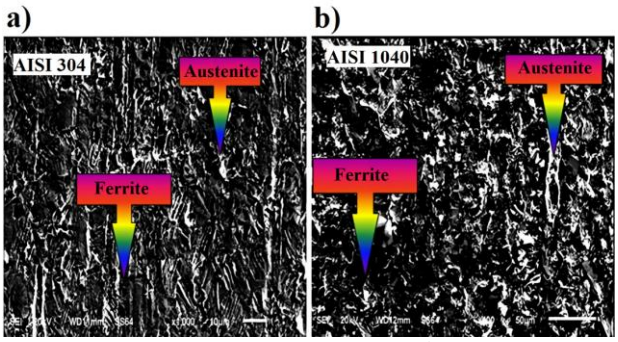

Figure 8. Microstructure SEM photographs of AISI 304 and AISI 1040 steel

SEM photographs of samples S1-S3, expressing the structural change, are shown in Figure 9. Structural changes in the weld area in the joints with different friction times and the effect of friction time on the structural change are seen. It has been observed that the width of the extremely deformed region at the weld interface in S1 and S2, due to the effect of temperature and pressure changes depending on the friction process. Microstructure grain quality is enhanced by friction welding. But, because of the combined influence of mechanical and thermal stresses, grains become thinner in the weld zone. It has been determined that the plastic deformation of austenitic-stainless steel AISI 304 has no effect on the friction welding variables or weld strength [18]. Increasing friction time can lead to the expansion of the high plastic deformation zone thus resulting in a hard zone at the joint interface [19]. Similar weld interfaces in Figure 9 were observed in the study of joining AISI 304 and AISI 1040 steels via friction welding conducted by [11].

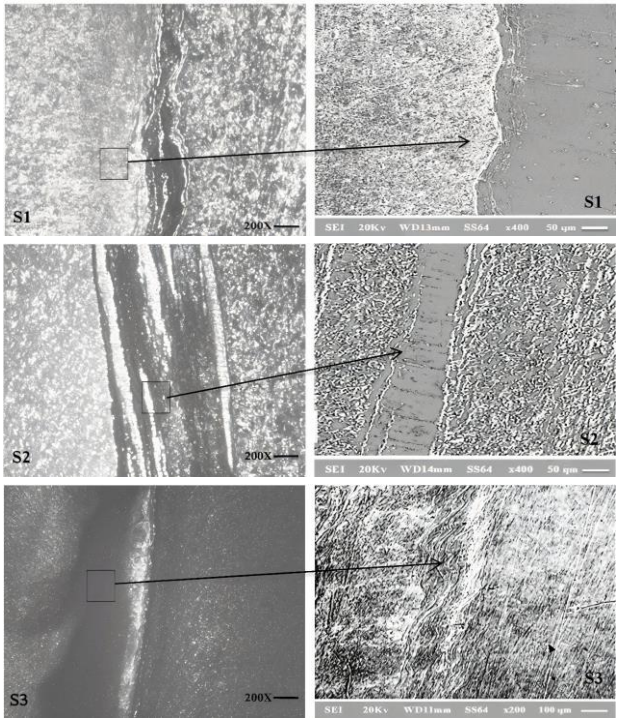

Figure 9. Optical and SEM images of samples S1, S2 and S3

Point EDS elemental analysis image on the weld cross-section of sample S3 is shown in Figure 10. The obtained results are given in Table 7. As can be seen from Table 1, the main steel material AISI 1040 contains almost no Cr, but AISI 304 contains 18.25 percent by weight. As can be seen from Table 7, in region 4, which is the weld region close to AISI 1040, there is an increase in the Cr rate, and in weld region 5 close to AISI 304, there is a decrease in the Cr rate. This is an indication of the mixing and diffusing of 304 and 1040 steels.

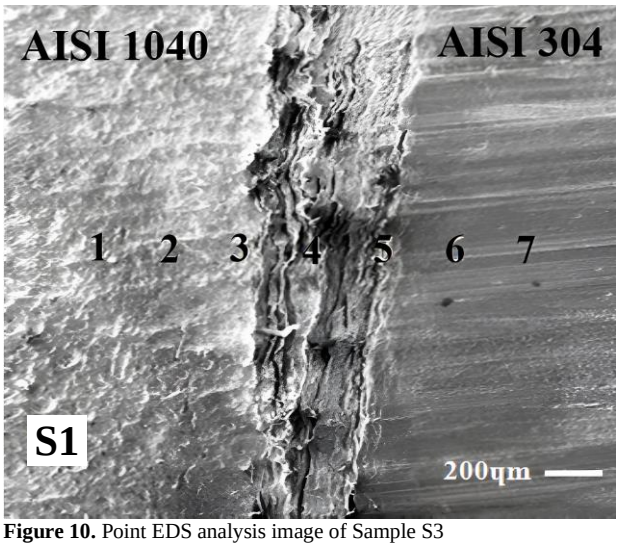

Figure 10. Point EDS analysis image of Sample S3

Figure 11 shows the XRD results of the S3 weld sample. Cr1.35Fe0.52, Cr23C6, Fe3C, and austenite phases were detected. In similar studies [20-23], ferrite, retained austenite and chromium (Cr) phases were formed in the weld. It is considered that the austenite phase occurs at ferrite grain boundaries and within the grain. The absence of XRD patterns of other phases such as carbides in the weld region means the welding process did not provide sufficient time for carbide formation [23].

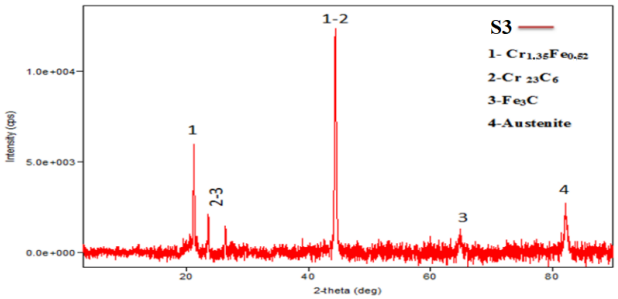

Figure 11. XRD graph of sample S3

Table 7. EDS values taken from 7 regions of the S3 sample

Elt.	Line	Units	1. AISI 1040 Main Material	2. HAZ Area	3. Deformed Area	4.Weld Area	5. Deformed Area	6. HAZ Area	7. AISI 304 Main Material
C	Ka	wt.%	0.000	0.000	0.000	0.000	0.000	0.000	0.000
Si	Ka	wt.%	0.449	1.285	0.503	0.237	0.129	0.594	0.473
Cr	Ka	wt.%	0.073	0.097	4.101	10.923	11.165	18.600	18.722
Mn	Ka	wt.%	0.675	0.709	1.570	2.432	2.249	1.405	1.461
Fe	Ka	wt.%	98.703	97.855	93.483	73.420	85.659	71.428	71.464
Ni	Ka	wt.%	0.099	0.054	0.342	2.988	0.798	7.974	7.880
		wt.%	100.000	100.000	100.000	100.000	100.000	100.000	100.000

3.3. Tensile Strength Test Results

The tensile strength diagram drawn according to the results obtained is shown in Figure 12. Sample S3 had the highest tensile strength and elongation while S1 had the lowest tensile strength and elongation. It has been observed that tensile strength and elongation increase with the increase in the friction time. The error bars for the tensile strength of the welded samples are provided in Figure 13. Three tensile tests were performed for each sample. Average tensile strengths of 661, 696 and 755 MPa for S1, S2 and S3, respectively. Celik et al. [11] joined AISI 304 and AISI 1040 different steels using friction welding and produced the weld with the highest tensile strength of an average of 792.4 MPa. Paventhan et al. [12] also investigated friction welding AISI 1040 and AISI 304 steels by optimizing welding parameters of friction time, friction pressure, forging pressure, and forging time. According to the results obtained, the strongest weld with a tensile strength of 543 MPa in which 6 s friction time was used. It was also concluded that friction time has the most effect on weld strength than other welding parameters.

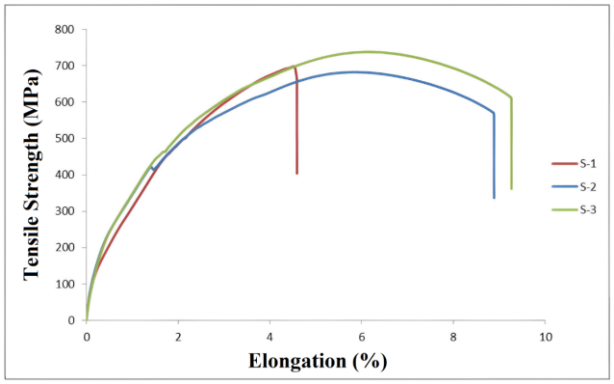

Figure 12. Stress-strain curves of S1, S2, S3 welded samples

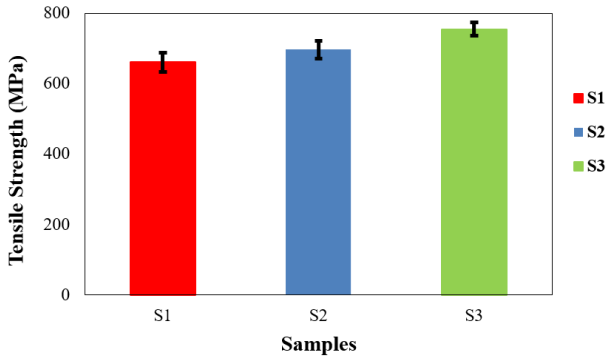

Figure 13. Tensile strength of the welded samples

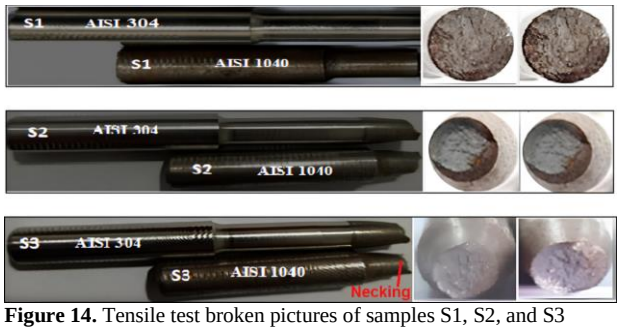

Figure 14. Tensile test broken pictures of samples S1, S2, and S3

When the broken surface photographs sample S1 are examined in Figure 15, some dimples and cleavages can be seen, meaning a mix of ductile and brittle fracture occurred. Tensile strength test broken pictures of samples S1, S2, and S3 are shown in Figure 14, it can be seen that there is necking in S2 and S3, but almost straight fracture perpendicular to the load direction for S1. It is evident from Figure 12 and the necking fracture in Figure 14 that S2 and S3 fracture ductile. All the samples failed from the welded areas. Celik et al. [11] examined the friction weld tensile fracture surface of the 1040 and 304 steels and determined the signs indicating brittle and ductile fractures.

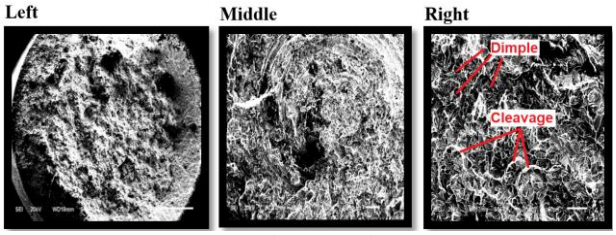

Figure 14. SEM photos taken from the left, middle, and right sides of the tensile fractured surface of sample S1

3.4. Microhardness Test Results

The results of the microhardness tests are given graphically in Figure 15. It was observed that the hardness value in the AISI 304 heat-affected region (HAZ) region decreased. The highest hardness values were in the weld areas due to deformation hardening with martensite formation upon sudden cooling. The hardness in the weld area decreased slightly with increasing of friction time. The hardness values at the weld zone of welds S1, S2 and S3 were found to be approximately 310, 270 and 240 HV, respectively. So, the lowest hardness value was obtained in the weld sample S3. This is probably due to the S3 having the highest friction time and thus heat input resulting in softening. Similar results were reported by [24, 25]. Higher friction time caused higher heat input. According to Ekinci and Balalan [26], higher heat input caused

larger grains in the microstructure, leading to softening. Celik et al. [11] found that the microhardness of HAZ regions was lower compared to the weld zones having microhardness values ranging between 210 and 260 HV for friction welding of dissimilar AISI 304 and AISI 1040 steels. The increase in the hardness of the weld zone was attributed to the Cr transformation from AISI 304 to AISI 1040 side, resulting in the formation of chromium-carbide by heat. In this study, Cr transformation was also seen in Table 7.

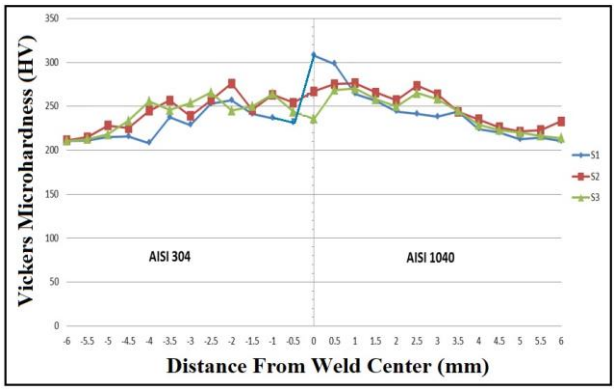

Figure 15. Microhardness distribution of the samples (S1, S2 and S3) on the horizontal axis

4. CONCLUSIONS

In the joining of dissimilar AISI 304 and AISI 1040 steels by friction welding, 3 different friction times (5, 7 and 9 seconds) were used and the influence of friction time on the mechanical and microstructural properties of the weld was determined. Accordingly,

1. It has been found that the surface temperature taken from the surface of welded joints increases in parallel with the increase of friction time.
2. The highest tensile stress of 755 MPa was seen in the S3 sample having the highest friction time while the lowest tensile stress of 661 MPa was determined in the S1 sample with the lowest friction time. The tensile strength and also elongation of the weld increased by increasing friction time.
3. Microhardness values around 310, 270 and 240 HV were reached at the joint areas of S1, S2 and S3 welds, respectively.
4. A decrease in the hardness value at the weld interface was observed when the friction time was increased.
5. It has been observed that the width and shape of the excessively deformed region on both sides of the joint interface changed due to the effect of temperature and pressure depending on the friction time.
6. S2 and S3 weld samples exhibited a ductile fracture during the tensile strength test. However, S1 weld sample was broken as a mixture of brittle and ductile.

REFERENCES

[1] Dahlan H, Nasution AK, Rusli M. Preliminary study on effect of inertia and continuous friction welding on mechanical properties of SS 316-Zn alloys friction welded joint. Journal of Advanced Joining Processes. 2024;9:100187.

[2] Kumar Rajak D, Pagar DD, Menezes PL, Eyvazian A. Friction-based welding processes: friction welding and friction stir welding. J. Adhes Sci.. Technol. 2020;34(24):2613-2637.

[3] Mortezaie A, Shamanian M. An assessment of microstructure, mechanical properties and corrosion resistance of dissimilar welds between Inconel 718 and 310S austenitic stainless steel. International Journal of Pressure Vessels and Piping. 2014;116:37-46.

[4] Dinc D. Investigation of weldability of AISI 1020 and AISI 304 steels by friction welding. M.Sc. Thesis. Balıkesir University, Institute of Science, Balıkesir; 2006.

[5] Meshram SD, Mohandas T, Madhusudhan Reddy G. Friction welding of dissimilar pure metals. J Mater Process Technol 2008;184:330-337.

[6] Sathiya P, Aravindan S, Noorul Haq A. Some experimental investigations on friction welded stainless steel joints. Mater Des. 2007;29:1099-1109.

[7] Sahin M. Simulation of friction welding using a developed computer program. J Mater Process Technol. 2004;153(4):1011–8.

[8] Ekinci O. Effect of tool rotational speed on friction stir spot welds of AZ31B Mg alloy to AISI 304 stainless steel. Materials Testing. 2024;66(4):534-43.

[9] Ekinci O. Friction stir lap welding of AZ31B magnesium alloy to AISI 304 stainless steel. Materials Testing. 2024;66(9):1367-78.

[10] Balalan Z, Ekinci O. Effect of Rotation Speed Parameter on Mechanical Properties of Similar AISI 1040 Parts Joined by Friction Welding. Metallofiz. Noveishie Tekhnol. 2018;40(12):1699-707.

[11] Celik S, Dinc D, Yaman R, and Ay I. An Investigation on Weldability of AISI 304 and AISI 1040 Steels on Friction Welding. Practical Metallography. 2010;47(4):188-205.

[12] Paventhan R, Lakshminarayanan PR, Balasubramanian V. Optimization of Friction Welding Process Parameters for Joining Carbon Steel and Stainless Steel. Journal of Iron and Steel Research, International. 2012;19(1):66-71.

[13] Guo W, You G, Yuan G, Zhang X. Microstructure and mechanical properties of dissimilar inertia friction welding of 7A04 aluminum alloy to AZ31 magnesium alloy. J. Alloys Compd. 2017;695:3267-77.

[14] Pratyusha M, Ramana PV, Prasanthi G. Evaluation of tensile strength of dissimilar metal pure aluminium and pure copper friction welds. Mater. Today Proc. 2021;38:2271-74.

[15] Nasution AK, Nawangsari P, Junaidi A, Hermawan H. Friction welding of AZ31-SS316L for partially-

degradable orthopaedic pins. IOP Conf. Ser. Mater. Sci. Eng. 2019;532:012014.
[16] Dahlan H, Nasution AK, Zuhdi SA, Rusli M. Study of the effect of friction time and preheating on the joint mechanical properties of friction welded SS 316- Pure Zn. Appl. Sci. 2023;13(2):988.
[17] Adin MS, Okumuş M. Investigation of Microstructural and Mechanical Properties of Dissimilar Metal Weld Between AISI 420 and AISI 1018 Steels, Arabian Journal for Science and Engineering. 2022;47:8341-50.
[18] Sahin M. Characterization of properties in plastically deformed austenitic-stainless steels joined by friction welding. Materials & Design. 2009;30(1):135-44.
[19] Shi Y, Li W, Tian L, Sun Y, Zhang J, Zhao HJL, Xu L, Han Y. Effect of ferrite and grain boundary characteristics on corrosion properties of thermal simulated 316 L heat affected zone. Corrosion Science. 2023;222:111384.
[20] Kumar NN, Ram GJ, Bhattacharya S, Dey H, Albert S. Spark plasma welding of austenitic stainless steel AISI 304L to commercially pure titanium. Trans. Indian Inst. Met. 2015;68:289-97.
[21] Mohammed M, Omar M, Sajuri Z, Al-Zubaidi S. Characterization of metallurgical and mechanical properties of thixowelded AISI D2 and AISI 304 steels. J. Mater. Eng. Perform. 2020;29:739-49.
[22] Kumar AS, Khadeer SA, Rajinikanth V, Pahari S, Kumar BR. Evaluation of bond interface characteristics of rotary friction welded carbon steel to low alloy steel pipe joints. Materials Science and Engineering: A. 2021;824:141844.
[23] Saeidi K, Zapata DL, Lofaj F, Kvetkova L, Olsen J, Shen Z, et al. Ultra-high strength martensitic 420 stainless steel with high ductility. Addit. Manuf. 2019;29:100803.
[24] Fu L, Duan L. The coupled deformation and heat flow analysis by finite element method during friction welding. Welding journal. 1998;77(5):202-7.
[25] Sluzalec A. Thermal effects in friction welding. Int. J. Mech. Sci. 1990;32(6):467-78.
[26] Ekinci O, Balalan Z. Influence of tool pin shape and rotation speed for friction stir spot welding of AZ91 magnesium alloy sheets. Materials Testing. 2023;65(8):1281-91.